JOC Article
pubs.acs.org/joc

Characterization of the 4-(Benzothiazol-2-yl)phenylnitrenium Ion from a Putative Metabolite of a Model Antitumor Drug

Mrinal Chakraborty,[†] Kyoung Joo Jin,[†] Stephen A. Glover,[‡] and Michael Novak*[,†]

[†]*Department of Chemistry and Biochemistry, Miami University, Oxford, Ohio 45056, and* [‡]*Division of Chemistry, School of Science and Technology, University of New England, Armidale, 2351, New South Wales, Australia*

novakm@muohio.edu

Received June 29, 2010

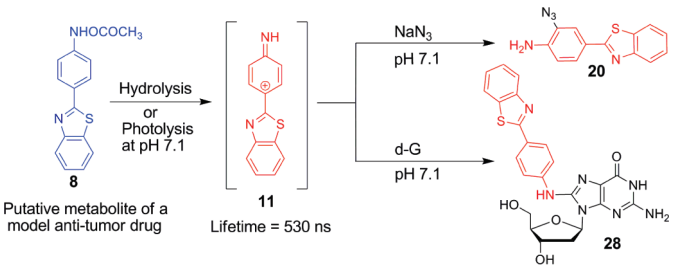

The 4-(benzothiazol-2-yl)phenylnitrenium ion **11** is generated from hydrolysis or photolysis of *O*-acetoxy-*N*-(4-(benzothiazol-2-yl)phenyl)hydroxylamine **8**, a model metabolite of 2-(4-aminophenyl)benzothiazole **1** and its ring-substituted derivatives that are being developed for a variety of medicinal applications, including antitumor, antibacterial, antifungal, and imaging agents. Previously, we showed that **11** had an aqueous solution lifetime of 530 ns, similar to the 560 ns lifetime of the 4-biphenylylnitrenium ion **12** derived from the well-known chemical carcinogen 4-aminobiphenyl. We now show that the analogy between these two cations extends well beyond their lifetimes. The initial product of hydration of **11** is the quinolimine **16**, which can be detected as a long-lived reactive intermediate that hydrolyzes in a pH-dependent manner into the final hydrolysis product, the quinol **15**. This hydrolysis behavior is equivalent to that previously described for a large number of ester metabolites of carcinogenic arylamines, including 4-aminobiphenyl. The major azide trapping product (90% of azide products) of **11**, **20**, is generated by substitution on the carbons *ortho* to the nitrenium ion center of **11**. This product is a direct analogue of the major azide adducts, such as **22**, generated from trapping of the nitrenium ions of carcinogenic arylamines. The azide/solvent selectivity for **11**, k_{az}/k_s, is also nearly equivalent to that of **12**. A minor product of the reaction of **11** with N_3^-, **21**, contains no azide functionality but may be generated by a process in which N_3^- attacks **11** at the nitrenium ion center with loss of N_2 to generate a diazene **25** that subsequently decomposes into **21** with loss of another N_2. The adduct derived from attack of 2′-deoxyguanosine (d-G) on **11**, **28**, is a familiar C-8 adduct of the type generated from the reaction of d-G with a wide variety of arylnitrenium ions derived from carcinogenic arylamines. The rate constant for reaction of d-G with **11**, $k_{d\text{-}G}$, is very similar to that observed for the reaction of d-G with **12**. The similar lifetimes and chemical reactivities of **11** and **12** can be rationalized by B3LYP/6-31G(d) calculations on the two ions that show that they are of nearly equivalent stability relative to their respective hydration products. The calculations also help to rationalize the different regiochemistry observed for the reaction of N_3^- with **11** and its oxenium ion analogue, **13**. Since **8** is the likely active metabolite of **1** and a significant number of derivatives of **1** are being developed as pharmaceutical agents, the similarity of the chemistry of **11** to that of carcinogenic arylnitrenium ions is of considerable importance. Consideration should be given to this chemistry in continued development of pharmaceuticals containing the 2-(4-aminophenyl)benzothiazole moiety.

Published on Web 07/16/2010 DOI: 10.1021/jo101275y

CHART 1

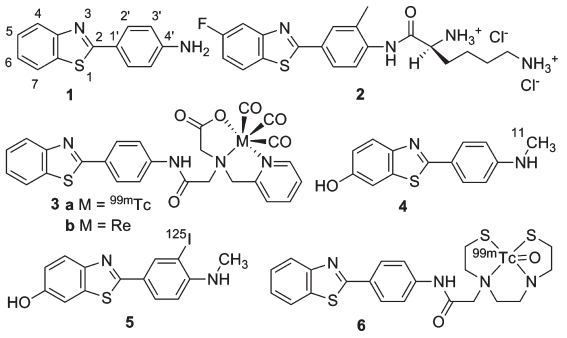

Introduction

In 1996, the antitumor activity of 2-(4-aminophenyl)-benzothiazole, **1** (Chart 1), and its ring-substituted derivatives was first reported.[1] The easily synthesized **1** was found to have remarkable activity against the human breast cancer cell lines MCF-7 (IC_{50} = 0.3−0.8 nM) and MDA 468 (IC_{50} = 1.6 nM).[1] Further work showed that a 3′-Me enhances antitumor activity and a 5-F suppresses metabolic deactivation of the drug.[2−4] The fluorinated water-soluble pro-drug, **2**, dubbed Phortress, was approved for phase 1 clinical trials in Britain in 2004.[5,6] Other compounds derived from **1** show significant in vitro and in vivo activity against human breast, colon, and renal cancer cell lines, and research on new compounds related to **1** continues to be reported.[7−9]

Complexes incorporating the 2-(4-aminophenyl)benzothiazole moiety, **3**, are being developed as radiopharmaceuticals for imaging (**3a**) and targeted radiotherapy (**3b**, ^{186}Re, ^{188}Re) of breast cancer.[10] Derivatives of **1**, including **4**−**6**, are being investigated as radiopharmaceuticals for binding and in vivo imaging of Aβ plaques, one of the earliest pathological processes in the development of Alzheimer's disease.[11−15] Other derivatives of **1** are under investigation as antimicrobial and antifungal agents.[16−18]

Metabolism of 2-(4-aminophenyl)benzothiazoles into the active metabolite in sensitive cell lines requires the constitutive presence of the 1A1 isoform of cytochrome P450, CYP1A1, that is also induced by the drug.[19] This activation also leads to detoxification since CYP1A1 hydroxylates the drug at the 6-position, leading to an inactive metabolite.[20] Metabolism of these compounds is associated with translocation of the aryl hydrocarbon receptor (AhR) to the nucleus, and metabolism is significantly attenuated in AhR-deficient MCF-7 cells.[21,22] The involvement of AhR binding in CYP1A1 induction by other xenobiotics is well-known.[23] On the basis of the available data, the mechanism of action of **1** and its simple ring-substituted derivatives is thought to involve selective uptake into sensitive cells followed by AhR binding and translocation into the nucleus, induction of CYP1A1, oxidation and conversion of the drug into an electrophilic reactive intermediate, and formation of extensive DNA adducts resulting in cell death.[6] It is suspected that the active metabolite of **1** is the hydroxylamine **7** or, more likely, an ester derivative, **8** or **9** (Scheme 1), but these compounds had not been reported in the literature.[6,24] The diacetylated derivative **10** has been reported and shown to be active against some of the same cell lines as **1**.[20] It has not been studied further because its high reactivity makes conclusions from bioassay studies difficult to interpret.[20] DNA adducts are known to be formed, and single and double DNA strand breaks have been reported, but the structures of DNA adducts have not been determined.[24−28] It has been proposed that the nitrenium ion **11** (Scheme 2) is responsible for the antitumor activity of **1**, but no direct evidence was provided.[24,29,30]

(1) Shi, D.-F.; Bradshaw, T. D.; Wrigley, S.; McCall, C. J.; Lelieveld, P.; Fichtner, I.; Stevens, M. F. G. *J. Med. Chem.* **1996**, *39*, 3375–3384.
(2) Bradshaw, T. D.; Wrigley, S.; Shi, D.-F.; Schultz, R. J.; Paull, K. D.; Stevens, M. F. G. *Br. J. Cancer* **1998**, *77*, 745–752.
(3) Bradshaw, T. D.; Shi, D.-F.; Schultz, R. J.; Paull, K. D.; Kelland, L.; Wilson, A.; Garner, C.; Fiebig, H. H.; Wrigley, S.; Stevens, M. F. G. *Br. J. Cancer* **1998**, *78*, 421–429.
(4) Hutchinson, I.; Chua, M.-S.; Browne, H. L.; Trapani, V.; Bradshaw, T. D.; Westwell, A. D.; Stevens, M. F. G. *J. Med. Chem.* **2001**, *44*, 1446–1455.
(5) Hutchinson, I.; Jennings, S. A.; Vishnuvajjala, B. R.; Westwell, A. D.; Stevens, M. F. G. *J. Med. Chem.* **2002**, *45*, 744–747.
(6) (a) Bradshaw, T. D.; Westwell, A. D. *Curr. Med. Chem.* **2004**, *11*, 1009–1021. (b) Weekes, A. A.; Westwell, A. D. *Curr. Med. Chem.* **2009**, *16*, 2430–2440.
(7) Hutchinson, I.; Bradshaw, T. D.; Matthews, C. S.; Stevens, M. F. G.; Westwell, A. D. *Bioorg. Med. Chem. Lett.* **2003**, *13*, 471–474.
(8) (a) Mortimer, C. G.; Wells, G.; Crochard, J.-P.; Stone, E. L.; Bradshaw, T. D.; Stevens, M. F. G.; Westwell, A. D. *J. Med. Chem.* **2006**, *49*, 179–185. (b) Aiello, S.; Wells, G.; Stone, E. L.; Kadri, H.; Bazzi, R.; Bell, D. R.; Stevens, M. F. G.; Matthews, C. S.; Bradshaw, T. D.; Westwell, A. D. *J. Med. Chem.* **2008**, *51*, 5135–5139.
(9) (a) Mukherjee, A.; Martin, S. G. *Int. J. Oncol.* **2006**, *29*, 1287–1294. (b) Akhtar, T.; Hameed, S.; Al-Masoudi, N. A.; Loddo, R.; La Colla, P. *Acta Pharm.* **2008**, *58*, 135–149.
(10) (a) Tzanopoulou, S.; Pirmettis, I. C.; Patsis, G.; Paravatou-Petsotas, M.; Livaniou, E.; Papadopoulos, M.; Pelecanou, M. *J. Med. Chem.* **2006**, *49*, 5408–5410. (b) Tzanopoulou, S.; Sagnou, M.; Paravatou-Petsotas, M.; Gourni, E.; Loudos, G.; Xanthopoulos, S.; Lafkas, D; Kiaris, H.; Varvarigou, A.; Pirmettis, I. C.; Papadopoulos, M.; Pelecanou, M. *J. Med. Chem.* **2010**, *53*, 4633–4641.
(11) Wang, Y.; Klunk, W. E.; Debnath, M. L.; Huang, G.-F.; Holt, D. P.; Shao, L.; Mathis, C. A. *J. Mol. Neurosci.* **2004**, *24*, 55–62.
(12) Wu, C.; Cai, L.; Wei, J.; Pike, V. W.; Wang, Y. *Curr. Alzheimer Res.* **2006**, *3*, 259–266.
(13) Serdons, K.; Verduyckt, T.; Cleynhens, J.; Terwinghe, C.; Mortelmans, L.; Bormans, G.; Verbruggen, A. *Bioorg. Med. Chem. Lett.* **2007**, *17*, 6086–6090.
(14) Wu, C.; Wei, J.; Gao, K.; Wang, Y. *Bioorg. Med. Chem.* **2007**, *15*, 2789–2796.
(15) Henriksen, G.; Hauser, A. I.; Westwell, A. D.; Yousefi, B. H.; Schwaiger, M.; Drzezga, A.; Wester, H.-J. *J. Med. Chem.* **2007**, *50*, 1087–1089.
(16) Yildiz-Oren, I.; Yalcin, I.; Aki-Sener, E.; Ucarturk, N. *Eur. J. Med. Chem.* **2004**, *39*, 291–298.
(17) Zhou, Y.; Sun, Z.; Froelich, J. M.; Hermann, T.; Wall, D. *Bioorg . Med. Chem. Lett.* **2006**, *16*, 5451–5456.
(18) Ra, C. S.; Jung, B. Y.; Park, G. *Heterocycles* **2004**, *62*, 793–802.
(19) Chua, M.-S.; Kashiyama, E.; Bradshaw, T. D.; Stinson, S. F.; Brantley, E.; Sausville, E. A; Stevens, M. F. G *Cancer Res.* **2000**, *60*, 5196–5203.
(20) Kashiyama, E.; Hutchinson, I.; Chua, M.-S.; Stinson, S. F.; Phillips, L. R.; Kaur, G.; Sausville, E. A.; Bradshaw, T. D.; Westwell, A. D.; Stevens, M. F. G. *J. Med. Chem.* **1999**, *42*, 4172–4184.
(21) Loaiza-Perez, A. I.; Trapani, V.; Hose, C.; Singh, S. S.; Trepel, J. B.; Stevens, M. F. G.; Bradshaw, T. D.; Sausville, E. A. *Mol. Pharmacol.* **2002**, *61*, 13–19.
(22) Trapani, V.; Patel, V.; Leong, C.-O.; Ciolino, H. P.; Yeh, G. C.; Hose, C.; Trepel, J. B.; Stevens, M. F. G.; Sausville, E. A.; Loaiza-Perez, A. I. *Br. J. Cancer* **2003**, *88*, 599–605.
(23) Bradshaw, T. D.; Trapani, V.; Vasselin, D. A.; Westwell, A. D. *Curr. Pharm. Des.* **2002**, *8*, 2475–2490.
(24) O'Brien, S. E.; Browne, H. L.; Bradshaw, T. D.; Westwell, A. D.; Stevens, M. F. G.; Laughton, C. A. *Org. Biomol. Chem.* **2003**, *1*, 493–497.
(25) Leong, C.-O.; Gaskell, M.; Martin, E. A.; Heydon, R. T.; Farmer, P. B.; Bibby, M. C.; Cooper, P. A.; Double, J. A.; Bradshaw, T. D.; Stevens, M. F. G. *Br. J. Cancer* **2003**, *88*, 470–477.
(26) Brantley, E.; Trapani, V.; Alley, M. C.; Hose, C. D.; Bradshaw, T. D.; Stevens, M. F. G.; Sausville, E. A.; Stinson, S. F. *Drug Metab. Dispos.* **2004**, *32*, 1392–1401.
(27) Leong, C. O.; Suggitt, M.; Swaine, D. J.; Bibby, M. C.; Stevens, M. F. G.; Bradshaw, T. D. *Mol. Cancer Ther.* **2004**, *3*, 1565–1575.
(28) Brantley, E.; Antony, S.; Kohlhagen, G.; Meng, L.; Agama, K.; Stinson, S. F; Sausville, E. A.; Pommier, Y. *Cancer Chemother. Pharmacol.* **2006**, *58*, 62–72.

SCHEME 1. Probable Metabolism of 1

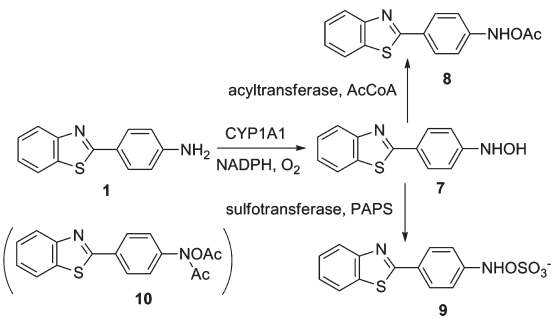

SCHEME 2. Nitrenium Ion 11 Generated from 8

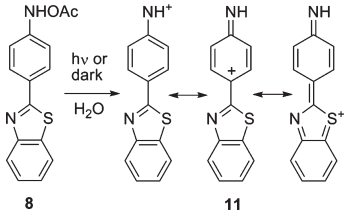

The proposed active metabolilites of **1** are consistent with the requirement of CYP1A1 for activation of the drug and with the well-known metabolism of carcinogenic arylamines into ester derivatives analogous to **8** and **9**.[31] The subsequent generation of nitrenium ions from the metabolites of arylamines and their reactions with DNA and other nucleophiles are now well documented.[32] Since the development of drugs and pharmaceuticals derived from **1** has been proceeding at a rapid pace, an understanding of the chemistry of its metabolites would be of interest, particularly due to the structural and metabolic similarity of **1** to well-known arylamine carcinogens. We recently reported the synthesis of **8** and demonstrated that hydrolysis or photolysis of this material (Scheme 2) led to a N_3^--trappable reactive intermediate identified as **11**.[33] Laser flash photolysis (lfp) of **8** led to the direct detection of **11** with λ_{max} = 570 nm and an aqueous solution lifetime of 530 ns. The effect of N_3^- on the kinetics of decay of **11** monitored at 570 nm was consistent with N_3^- trapping data obtained during hydrolysis of **8**, demonstrating that the same intermediate was generated during photolysis and hydrolysis.[33]

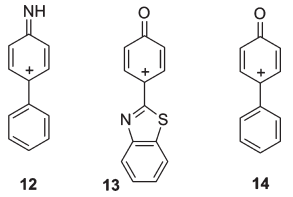

We now report the structures of the products of trapping **11** with N_3^- and 2′-deoxyguanosine (d-G) and a comparison

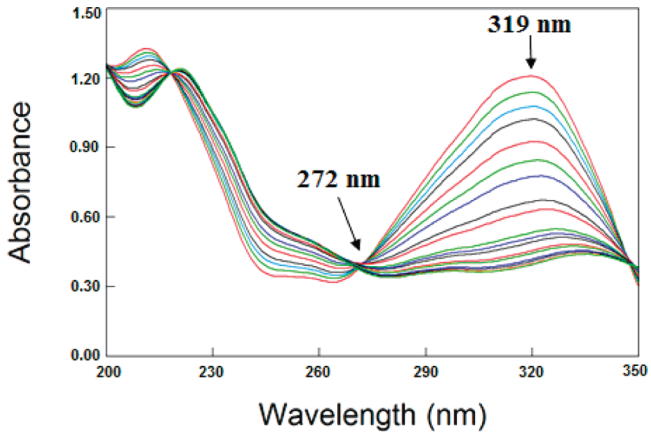

FIGURE 1. Repetitive wavelength scans taken during the decomposition of **8** in pH 7.1 buffer at 30 °C. Absorbance at 319 nm decreases with time. Delay between first and second scan is 60 s.

of the reactions of **11** with those of the 4-biphenylylnitrenium ion, **12**, derived from the carcinogen 4-aminobiphenyl.[34,35] The chemistry of **11** is also compared to that of the structurally related oxenium ions, **13** and **14**.[36,37] The results show that **11** behaves like a typical arylnitrenium ion derived from carcinogenic arylamines. Similarities and differences in the chemistry of **11**, **12**, and **13** can be rationalized by calculations on these ions performed at the B3LYP/6-31G(d) level of theory.

Results and Discusion

Kinetics of the Decomposition of 8. The repetitive wavelength scan of Figure 1 shows that **8** (λ_{max} = 319 nm) decomposes in pH 7.1 phosphate buffer (0.02 M total phosphate, 5 vol % CH_3CN-H_2O, μ = 0.5 ($NaClO_4$)) at 30 °C. The wavelength scan shows that an initial isosbestic point at ca. 272 nm does not hold throughout the course of the reaction, indicating the presence of a long-lived intermediate during the decomposition of **8**. Absorbance versus time data are fit best throughout the pH range of 1−8 by a double exponential rate equation consistent with two consecutive pseudo-first-order processes governed by the rate constants k_0 and k_1.[33,34a] Table S1 in the Supporting Information provides the rate constants collected at various wavelengths in the kinetics experiments. The final decomposition product throughout the pH range of 1−8 is the quinol **15** (Scheme 3). Kinetic data obtained by HPLC show that the decay of **8** is a first-order process, governed by the larger rate constant, k_0, while the appearance of **15** is biphasic and is fit well by the double exponential rate equation.[33] The larger rate constant generated by the fit is equivalent in magnitude to k_0 measured for the disappearance of **8** (Figure S1, Supporting Information). The rate of appearance of **15** is limited by the

(29) Hilal, R.; Khalek, A. A. A.; Elroby, S. A. K. *THEOCHEM* **2005**, *731*, 115–121.
(30) Stevens, M. F. G.; Shi, D.-F.; Castro, A. *J. Chem. Soc., Perkin Trans. 1* **1996**, 83–93.
(31) (a) Kim, D.; Guengerich, F. P. *Annu. Rev. Pharmacol.* **2005**, *45*, 27–49. (b) Guengerich, F. P. *Drug Metab. Rev.* **2002**, *34*, 607–623. (c) Beland, F. A.; Kadlubar, F. F. *Environ. Health Persp.* **1985**, *62*, 19–30.
(32) (a) Novak, M.; Rajagopal, S. *Adv. Phys. Org. Chem.* **2001**, *36*, 167–253. (b) Novak, M.; Rajagopal, S.; Xu, L.; Kazerani, S.; Toth, K.; Brooks, M.; Nguyen, T.-M. *J. Phys. Org. Chem.* **2004**, *17*, 615–624.
(33) Chakraborty, M.; Jin, K. J.; Brewer, S. C.; Peng, H.-L.; Platz, M. S.; Novak, M. *Org. Lett.* **2009**, *11*, 4862–4865.
(34) (a) Novak, M.; Kahley, M. J.; Eiger, E.; Helmick, J. S.; Peters, H. E. *J. Am. Chem. Soc.* **1993**, *115*, 9453–9460. (b) McClelland, R. A.; Davidse, P. A.; Hadzialic, G. *J. Am. Chem. Soc.* **1995**, *117*, 4173–4174.
(35) (a) Novak, M.; Kennedy, S. A. *J. Am. Chem. Soc.* **1995**, *117*, 574–575. (b) Kennedy, S. A.; Novak, M.; Kolb, B. A. *J. Am. Chem. Soc.* **1997**, *119*, 7654–7664.
(36) (a) Novak, M.; Glover, S. A. *J. Am. Chem. Soc.* **2004**, *126*, 7748–7749. (b) Wang, Y.-T.; Wang, J.; Platz, M. S.; Novak, M. *J. Am. Chem. Soc.* **2007**, *129*, 14566–14567.
(37) Wang, Y.-T.; Jin, K. J.; Myers, L. R.; Glover, S. A.; Novak, M. *J. Org. Chem.* **2009**, *74*, 4463–4471.

SCHEME 3. Decomposition of 8 with Comparison to the Model Carcinogens 17a and 17b

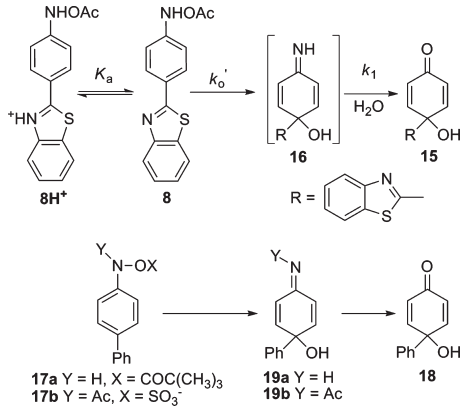

smaller rate constant, k_1. Kinetics of the appearance of **15** are consistent with its formation from a long-lived intermediate (lifetime ca. 2 h at pH 7.1 and 10 °C, ca. 30 min at pH 7.1 and 30 °C) that is generated by hydrolysis of **8**. This intermediate was not isolated, but its kinetic behavior and the structure of its final hydrolysis product **15** are most consistent with the quinolimine, **16**. The biphasic appearance of **15** is a result of the similar magnitudes of k_0 and k_1, which require that **16** builds up to significant concentrations during the reaction.[33] Similar long-lived quinolimines **19a**,**b** have been detected during the hydrolysis of the biphenylyl esters **17a**,**b** derived from the carcinogen 4-aminobiphenyl (Scheme 3).[34a] The final hydrolysis product of both **17a** and **17b** is the quinol **18**.[34a] This is a common reaction motif for hydrolysis of many esters of *N*-arylhydroxylamines and *N*-arylhydroxamic acids.[32,38]

The absorbance at 319 nm for **8** is pH-dependent, decreasing in magnitude at pH < 3.0. A plot of the initial absorbance of **8** at 319 nm versus pH (Figure S2, Supporting Information) was fit to a standard titration curve to obtain a pK_a of 1.45 ± 0.13. This pK_a is consistent with deprotonation of NH$^+$ on the thiazole ring system of **8H**$^+$ (Scheme 3).[39] The rate constant k_0 is also pH-dependent (Figure 2), decreasing at pH < 3.0. The pH dependence of k_0 is described by eq 1.

$$k_0 = k_0' K_a/(10^{-\mathrm{pH}} + K_a) \qquad (1)$$

This rate law is consistent with the spontaneous, uncatalyzed decomposition of **8** governed by k_0', while the conjugate acid **8H**$^+$ is unreactive under the hydrolysis conditions. Rate and equilibrium constants gathered from fitting the kinetic data are gathered in Table 1. The kinetic pK_a of 1.47 ± 0.04 is equivalent to the spectrophotometric pK_a measured at 319 nm. This rate law is equivalent to that observed for hydrolysis of a series of esters of hydroxylamines and hydroxamic acids derived from carcinogenic heterocyclic arylamines that can be protonated at a heterocyclic N.[32b]

(38) (a) Novak, M.; Pelecanou, M.; Roy, A. K.; Andronico, A. F.; Plourde, F. M.; Olefirowicz, J. M.; Curtin, T. J. *J. Am. Chem. Soc.* **1984**, *106*, 5623–5631. (b) Novak, M.; Roy, A. K. *J. Org. Chem.* **1985**, *50*, 571–580. (c) Novak, M.; Roy, A. K. *J. Org. Chem.* **1985**, *50*, 4884–4888.

(39) (a) Öğretir, C.; Demirayak, Ş.; Tay, N. F.; Duran, M. *J. Chem. Eng. Data* **2008**, *53*, 422–426. (b) Notario, R.; Herreros, M.; Ballesteros, E.; Essefar, M.; Abboud, J.-L. M.; Sadekov, I. D.; Minkin, V. I.; Elguero, J. *J. Chem. Soc., Perkin Trans. 2* **1994**, 2341–2344.

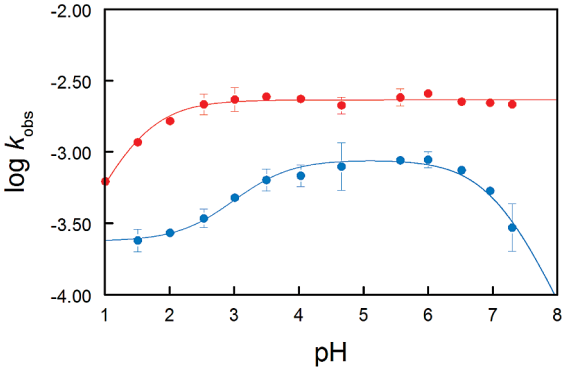

FIGURE 2. Profile of pH rate for k_0 (red) and k_1 (blue) at 30 °C. Data were fit by nonlinear least-squares procedure to eq 1 for k_0 and eq 2 for k_1.

TABLE 1. Derived Rate Parameters for 8, 11, and 16[a]

parameter	species	experimental method	value
pK_a[b]	**8**	UV titration	1.45 ± 0.13[e]
pK_a[b]	**8**	UV	1.47 ± 0.04[f]
k_0[b]	**8**	UV	$(2.31 \pm 0.05) \times 10^{-3}$ s^{-1}[f]
pK_{a1}[c]	**16**	UV	3.28 ± 0.11
pK_{a2}[c]	**16**	UV	7.07 ± 0.06
k_1'[c]	**16**	UV	$(8.8 \pm 0.4) \times 10^{-4}$ s^{-1}
k_1''[c]	**16**	UV	$(2.4 \pm 0.2) \times 10^{-4}$ s^{-1}
k_s[d]	**11**	lfp, UV	$(1.87 \pm 0.07) \times 10^{6}$ s^{-1}[g]
k_{az}[d]	**11**	lfp, UV	$(4.94 \pm 0.17) \times 10^{9}$ M^{-1} s^{-1}[h]
$k_{d\text{-}G}$	**11**	competition	$(3.2 \pm 0.6) \times 10^{9}$ M^{-1} s^{-1}[i]

[a]Conditions: 5 vol % CH_3CN-H_2O, 30 °C, $\mu = 0.5$. [b]Defined in Scheme 3. [c]Defined in Scheme 4. [d]Defined in Scheme 5. [e]Obtained from a fit of initial absorbance to a standard titration equation. [f]Obtained by a fit to eq 1. [g]Obtained by a fit to eq 2. [h]See ref 33. [i]Obtained from $k_{d\text{-}G}/k_s$ (see Figure 5) and known value of k_s.

SCHEME 4. Kinetic Scheme for pH Dependence of k_1

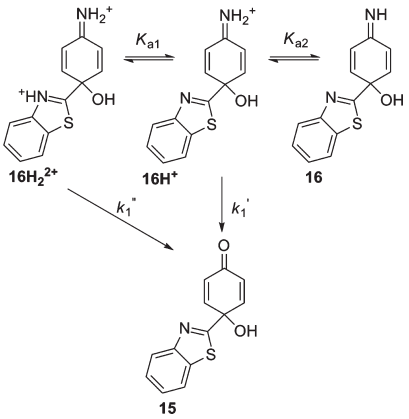

The rate constant k_1 that describes the hydrolysis of **16** into **15** exhibits pH dependence that can be fit to eq 2. This equation is derived from the kinetic mechanism of Scheme 4.

$$k_1 = (k_1''(10^{-\mathrm{pH}})^2 + k_1' K_{a1} 10^{-\mathrm{pH}})/(K_{a1}K_{a2} + K_{a1}10^{-\mathrm{pH}} + (10^{-\mathrm{pH}})^2) \qquad (2)$$

The parameters derived from the curve fitting are collected in Table 1. The results require that both **16H**$^+$ and **16H**$_2^{2+}$

SCHEME 5. Azide Trapping of 11 with Comparisons to 12

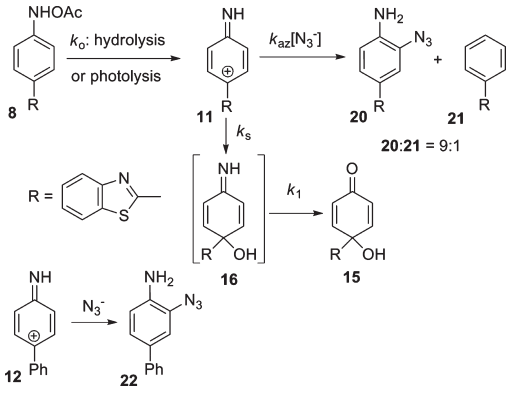

undergo hydrolysis to form **15**, with $\mathbf{16H}^+$ about 4-fold more reactive than its conjugate acid. No hydrolysis of the neutral species **16** could be detected, but the study was not extended to more basic pH, where hydrolysis of **16** may dominate. $\mathbf{16H_2}^{2+}$ is a somewhat weaker acid than expected. This could be due to stabilization of the thiazole NH^+ by solvation with the intramolecular OH group. Hydrolyis of related imines including **19a**,**b** occur with similar pH dependence.[32,34a]

The hydrolysis behavior of **8** is qualitatively very similar to that of esters of carcinogenic *N*-arylhydroxylamines that have been shown to generate nitrenium ion intermediates, but by themselves, these kinetic and product data cannot implicate a nitrenium ion **11** in the hydrolysis reaction of **8**. Trapping of **11** with N_3^- during hydrolysis, coupled with the direct detection and kinetic characterization of the same intermediate during lfp experiments, provides the necessary evidence for the involvement of the nitrenium ion during hydrolysis.[33]

Azide Trapping and Direct Detection of 11. We previously reported that addition of N_3^- ($\leq$5 mM) during hydrolysis of **8** generates two new products at the expense of the solvent-derived product **15**.[33] This product redistribution occurs without change in the rate of disappearance of **8**, implicating the involvement of a cationic intermediate generated by rate-limiting ionization of **8**.[33] Analysis of product yields obtained by HPLC methods led to a N_3^-/solvent selectivity, k_{az}/k_s, of $(2.6 \pm 0.3) \times 10^3$ M^{-1}. The lfp experiments on **8** generated a reactive intermediate with λ_{max} = 570 nm that decayed in a [N_3^-]-dependent pseudo-first-order fashion.[33] The directly measured rate constants k_{az} and k_s (Table 1) led to k_{az}/k_s of $(2.64 \pm 0.13) \times 10^3$ M^{-1}, identical to k_{az}/k_s obtained from the azide clock experiments. This demonstrated that the same reactive intermediate with an aqueous solution lifetime, $1/k_s$, of 530 ns was generated in both experiments.[33]

The products derived from N_3^- trapping have now been identified as **20** and **21** (Scheme 5). The major product **20** has a structure analogous to azide adducts derived from the trapping of nitrenium ions of carcinogenic amines.[32,34a] The azide adduct derived from **12** is the directly analogous compound **22**.[34a] The minor product **21** (ca. 10% of "azide adducts") is surprising. There is no azide moiety in its structure, but **21** is only generated when N_3^- is present. Its yield depends on [N_3^-] in the same way that the yield of **20** does, so it is generated by reaction of N_3^- with **11**.[33]

SCHEME 6. Possible Route to 21

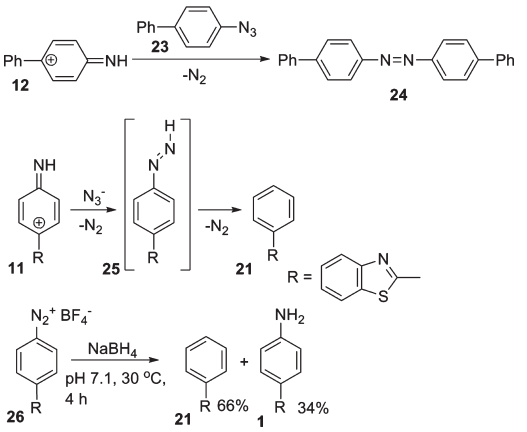

Recently, Phillips and co-workers have shown that photolytically generated **12** reacts with 4-biphenyl azide **23** at relatively high concentrations of **23** (ca. 1 mM), with loss of N_2, to yield *cis*- and *trans*-4,4′-azobisbiphenyl **24** (Scheme 6).[40] A similar reaction of **11** with N_3^- would yield the diazene **25**. Aryldiazenes are known to spontaneously decompose into the corresponding arene with loss of N_2.[41] This would provide a mechanism for generation of **21**. Since diazonium salts can be reduced to diazenes with $NaBH_4$,[41] we tested the plausibility of this path by reduction of the diazonium salt **26** with excess $NaBH_4$ in the pH 7.1 phosphate buffer used for our studies. Under these conditions, **21** was generated in 66% yield with **1** accounting for the rest of the product mixture. It is not clear how **1** is generated, but the substantial yield of **21** suggests that **25** decomposes into **21** under our reaction conditions. This experiment does not prove the pathway proposed in Scheme 6, but it does show that the last step is plausible. Although **21** is a minor product of the reaction of N_3^- with **11**, it was readily detected. If analogous products had been generated in similar yield from the reaction of other arylnitrenium ions with N_3^-, they would have been detected, although small amounts (ca. 1% yield) may have escaped detection.[32,34]

The aqueous solution lifetime of **11** is almost identical to that of **12** (530 ns for **11** and 560 ns for **12** under the same conditions), k_{az}/k_s is nearly the same for both cations (2.6×10^3 M^{-1} for **11** and 2.9×10^3 M^{-1} for **12**), and the products from reaction with the aqueous solvent and N_3^- are, with the exception of **21**, directly analogous.[34] The 4-(benzothiazol-2-yl) substituent stabilizes an arylnitrenium ion to the same extent as a 4-phenyl substituent once the ion is fully formed,[33] but a comparison of the rate constants for formation of **11** from **8** and **12** from **17a** in aqueous solution (2.3×10^{-3} s^{-1} at 30 °C for **8** vs 0.13 s^{-1} at 0 °C for **17a**[34a]) shows that the 4-(benzothiazol-2-yl) substituent destabilizes the transition state for N−O bond heterolysis relative to the 4-phenyl substituent by a factor of ca. 100-fold. An electron-withdrawing inductive effect of the 4-(benzothiazol-2-yl) substituent dominates until the cation is fully formed. We previously noted a similar situation for the oxenium ions **13** and **14**.[37]

(40) Xue, J.; Du, Y.; Guan, X.; Guo, Z.; Phillips, D. L. *J. Phys. Chem. A* **2008**, *112*, 11582–11589.

(41) (a) Huang, P. C.; Kosower, E. M. *J. Am. Chem. Soc.* **1968**, *90*, 2367–2376. (b) McKenna, C. E.; Traylor, T. G. *J. Am. Chem. Soc.* **1971**, *93*, 2313–2314.

SCHEME 7. Reaction of 13 with N_3^-

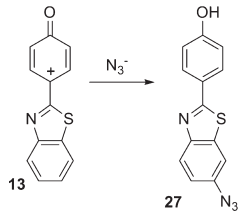

These two ions have comparable aqueous solution lifetimes and k_{az}/k_s, but generation of **13** and **14** from similar precursors (4-acetoxy-4-substituted-2,5-cyclohexadien-1-ones) occurs much more readily for **14**.[37] The retarding effect of the 4-(benzothiazol-2-yl) substituent on the rate of formation of both **11** and **13** is consistent with the previously measured σ_p of 0.29 for this substituent determined from its effect on the ionization constants of substituted benzoic acids.[42] The σ^+ for this substituent does not appear to have been previously measured, but our results for **11** and **13** suggest that its ability to stabilize a positive charge with which it is in resonance is similar to that of a phenyl substituent.

Regioselectivity of the Reaction of 11 and 13 with N_3^-. The major N_3^- adduct isolated from the oxenium ion **13** is **27** (Scheme 7).[37] Although both **11** and **13** react at or near the diffusion limit with N_3^-, there is considerable difference in the regioselectivity of the two reactions. Calculations at the B3LYP/6-31G(d) level provide some insight into this difference. Figure 3 provides a summary of the results for the calculations on **11** with comparisons to calculated results for **13** that were previously reported.[37]

11 exists in two isomeric forms depending upon the orientation of the N−H bond, which can be *syn* or *anti* to the sulfur atom in the heterocyclic ring. Both forms are planar, and the *anti* form is marginally more stable by 0.24 kcal/mol at the B3LYP/6-31G(d) level. **13** is also calculated to be planar at this level of theory.[37] Figure 3 shows that there are considerable similarities in the overall charge distribution and structure of the two cations, but there are also some striking differences. The positive charge is more delocalized into the benzothiazole ring in **13**; the overall charge on the atoms of the benzothiazole ring in **11** is +0.38 compared to +0.47 for **13**. Bond alternation is stronger in the phenyl ring of **13**, and the (C-4′)−(C-2) bond length is shorter in **13**, consistent with the smaller transfer of charge into the benzothiazole ring of **11**. In terms of a valence bond description, the resonance structures II−V are important contributors to both ions, but III−V are somewhat less important for **11**.

In agreement with the conclusions reached from Mulliken charges and bond lengths, the electron density electrostatic potential (EDEP) surfaces for **11** and **13** at the same iso level (Figure 4) show decreased delocalization of the positive charge into the benzothiazole ring of **11** compared to **13**. A comparison of the LUMOs of both cations (Figure S3, Supporting Information) shows relatively larger coefficients on the benzothiazole ring at N, S, C-4, and C-6 of **13**.

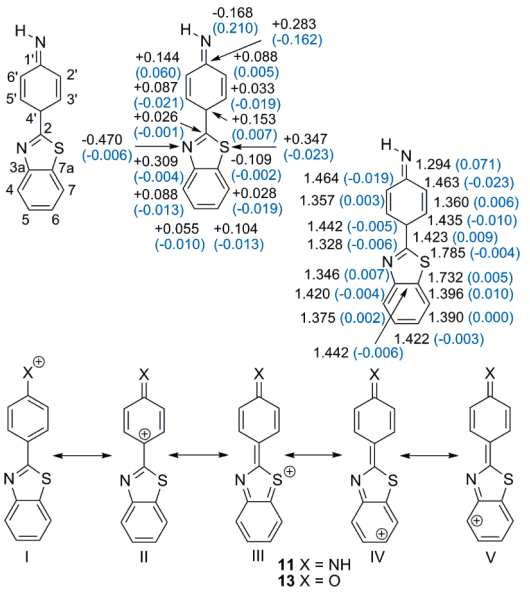

FIGURE 3. Charges and bond lengths computed at the B3LYP/6-31G(d) level for **11** (charges on H summed into heavy atoms). Data in blue correspond to the differences in charges or bond lengths for **11** and **13**. Resonance forms for **11** and **13** are also shown.

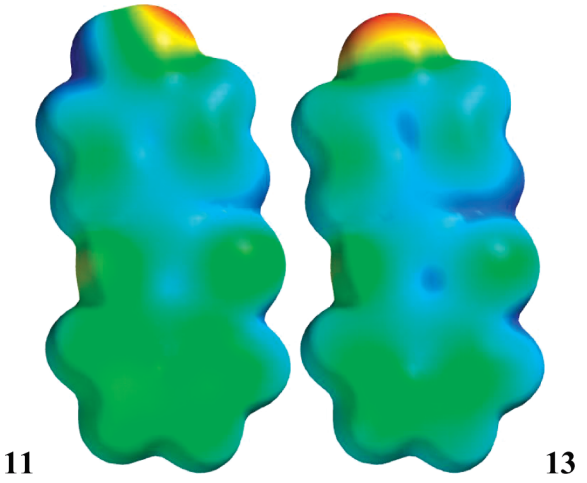

FIGURE 4. EDEP surfaces at 0.002 electrons/au^3 for **11** and **13**. The NH or O is at the top and S to the right in both surfaces.

The computational picture for the two ions suggests that both species are highly delocalized, but with somewhat less charge delocalization into the distal benzothiazole ring of **11**. The different regioselectivities exhibited by both ions for reaction with N_3^- are consistent with that picture.

Computed Relative Stabilities of 11, 12, 13, and 14. Isodesmic reactions involving nitrenium and oxenium ions and their quinol or quinolimine hydration products have been utilized to rationalize experimental differences in the lifetimes and selectivities of these cations.[37,43,44] Direct measurement on the cations after generation by lfp and azide

(42) (a) Bystrov, V. F.; Belaya, Zh. N.; Gruz, B. E.; Syrova, G. P.; Tolmachev, A. I.; Shulezhko, L. M.; Yagupol'skii, L. M. *Zh. Obshchei Khim.* **1968**, *38*, 1001–1005. (b) Durmis, J.; Karvas, M.; Manasek, Z. *Collect. Czech. Chem. Commun.* **1973**, *38*, 215–223.

(43) (a) Novak, M.; Lin, J. *J. Org. Chem.* **1999**, *64*, 6032–6040. (b) Glover, S. A.; Novak, M. *Can. J. Chem.* **2005**, *83*, 1372–1381. (c) Novak, M.; Poturalski, M. J.; Johnson, W. L.; Jones, M. P.; Wang, Y.-T.; Glover, S. A. *J. Org. Chem.* **2006**, *71*, 3778–3785.

(44) Novak, M; Glover, S. A. *J. Am. Chem. Soc.* **2004**, *126*, 7748–7749.

clock data shows that the lifetimes of **11** and **12** are nearly identical.[33,34] Likewise, **13** and **14** appear to have very similar lifetimes based on azide clock measurements, although **13** and **14** are considerably shorter-lived species than are **11** and **12**.[37,44] The ΔE values for the isodesmic equations (eqs 3−5) show the relative stabilities of these cations with respect to their initial quinolimine or quinol hydration products. ZPE corrections are not included because these corrections have been shown to have little effect on the results.[37,43,44]

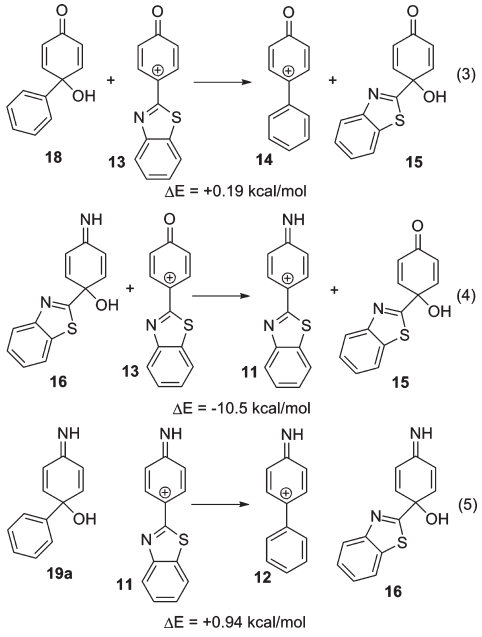

The result for eq 3 was previously reported and is included here for comparison purposes.[37] It shows that the two oxenium ions **13** and **14** are of almost equivalent stability relative to their respective hydration products. This would lead to similar lifetimes of these two cations in aqueous solution if the lifetimes are governed by the thermodynamic stability of the cations relative to their reaction products in water. This has been observed to be the case in previous correlations.[43a] Experimentally observed lifetimes based on azide clock measurements are 20 ns for **13** at 80 °C and 12 ns for **14** at 30 °C.[37,44] The two ions do have similar aqueous solution lifetimes. ΔE of eq 4 indicates that the nitrenium ion **11** is considerably more stable than its oxenium ion analogue **13**. This result is in good agreement with previous calculations of the relative stabilities of **12** and **14** that showed **12** is more stable than **14** relative to their hydration products by 11−13 kcal/mol at various levels of theory.[43b] In accord with the calculations, the lifetime for **11** of 530 ns is ca. 30-fold larger than that of **13**. Similar lifetime differences have previously been observed for a series of 4′-substituted 4-biphenylylnitrenium and the corresponding oxenium ions in water.[43c] The isodesmic calculation of eq 5 indicates that **11** and **12** are of very similar stability. The observed lifetimes of these two cations (530 ns for **11** and 560 ns for **12**) are in agreement with the prediction of eq 5. Both the experimental lifetime measurements and the calculations agree that **11** and **12** are very similar in stability and that the 4-(benzothiazol-2-yl) and 4-phenyl substituents have very similar effects on nitrenium ion stability.

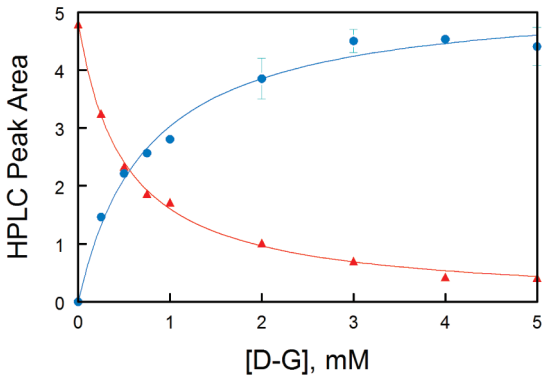

FIGURE 5. Yields of the quinol **15** (red) and the d-G adduct **28** (blue) as a function of [d-G] in pH 7.1 phosphate buffer at 30 °C. Data were fit to the standard azide clock equations.

Reaction of 11 with d-G. The decomposition of **8** in the presence of d-G in pH 7.1 phosphate buffer at [d-G] ≤ 10 mM leads to the formation of a single product **28** at the expense of the normal hydrolysis product **15** (Figure 5). At [d-G] ≥ 2.5 mM (≥80% trapping), the kinetics of disappearance of **8** monitored by UV absorbance conforms to a simple first-order pattern and the rate constant for the disappearance of **8** is equivalent to k_0 measured under the same conditions in the absence of d-G (Table S1, Supporting Information). This evidence shows that d-G efficiently traps the nitrenium ion **11** after rate-limiting ionization of **8**.

The product yield data were fit to the standard azide clock equations[33,45] to obtain the d-G/solvent selectivity ratio, $k_{d\text{-}G}/k_s$, of $(1.7 \pm 0.3) \times 10^3$ M^{-1}. Since k_s under these conditions is known from direct measurement (Table 1), $k_{d\text{-}G}$, the rate constant for the reaction of **11** with d-G, is $(3.2 \pm 0.6) \times 10^9$ M^{-1} s^{-1}. This rate constant is in the range expected for the diffusion-controlled reaction of an arylnitrenium ion with d-G and is similar in magnitude to the rate constant for the reaction of **12** with d-G of 2.0×10^9 M^{-1} s^{-1}.[46,47]

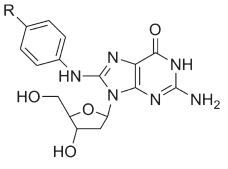

28 R = benzothiazol-2-yl
29 R = Ph

The product **28** is a C-8 adduct typical of the major products of reaction of other arylnitrenium ions with d-G.[46,48] For example, the only product isolated from the reaction of d-G with **12** is **29**.[46] The ions **11** and **12** react with d-G with almost identical rate constants to generate the same type of adduct. The evidence obtained from reaction products and

(45) Richard, J. P.; Jencks, W. P. *J. Am. Chem. Soc.* **1982**, *104*, 4689−4691; **1982**, *104*, 4691−4692; **1984**, *106*, 1383−1396.
(46) (a) Novak, M.; Kennedy, S. A. *J. Am. Chem. Soc.* **1995**, *117*, 574–575. (b) Kennedy, S. A.; Novak, M.; Kolb, B. A. *J. Am. Chem. Soc.* **1997**, *119*, 7654–7664.
(47) McClelland, R. A.; Gadosy, T. A.; Ren, D. *Can. J. Chem.* **1998**, *76*, 1327–1337.
(48) (a) Beland, F. A; Miller, D. W.; Mitchum, R. K. *J. Chem. Soc., Chem. Commun.* **1983**, 30–31. (b) Bosold, F.; Boche, G. *Angew. Chem.* **1990**, *102*, 99–100.

kinetics measurements shows that the 4-(benzothiazol-2-yl)-phenylnitrenium ion **11** behaves like a typical nitrenium ion derived from a carcinogenic arylamine.

Conclusion

The 4-(benzothiazol-2-yl) substituent slows the decomposition of **8** to generate the nitrenium ion **11** by a factor of ca. 100-fold compared to the 4-phenyl substituent of **17a**. Nevertheless, once the cation is generated, the 4-(benzothiazol-2-yl) substituent plays a very similar role to that of the 4-phenyl substituent. The two cations **11** and **12** have nearly identical aqueous solution lifetimes and chemical reactivities with N_3^- and d-G and generate analogous products from their reactions with those two nucleophiles, as well as with the aqueous solvent. The only exception to this chemical analogy is the minor reaction product **21** generated as ca. 10% of the mixture from the reaction of **11** with N_3^-. The cation **11** has chemical properties that are essentially equivalent to those of nitrenium ions derived from carcinogenic arylamines. Since **8** is the likely active metabolite of **1** and a significant number of derivatives of **1** are being developed as antitumor, antibacterial, and antifungal agents, and as in vivo imaging agents, the similarity of the chemistry of **11** to that of carcinogenic arylnitrenium ions is of considerable importance. Consideration should be given to this chemistry in continued development of pharmaceuticals containing the 2-(4-aminophenyl)benzothiazole moiety. We are continuing our studies with an emphasis on the reactions of **11** with other biological nucleophiles and on the effects of simple ring substituents on the chemistry of **11**.

Experimental Section

The synthesis and characterization of **8**, detection of **15** as the major hydrolysis product of **8**, the reaction conditions, HPLC experiments, and kinetics methodology have been described previously.[33]

Azide-Derived Products. A pH 7.1, 0.02 M phosphate buffer (500 mL, 5 vol % CH_3CN-H_2O, μ = 0.5 ($NaClO_4$)) containing 20 mM NaN_3 was incubated at 30 °C, while 20 mL of a 25 mM solution of **8** in CH_3CN was added in 1 mL portions every 10 min. After the last addition, the reaction mixture was incubated for 1.5 h. Products were extracted from the buffer with CH_2Cl_2 (3 × 100 mL). The combined extracts were dried (Na_2SO_4), filtered, and rotary evaporated to obtain a brown solid. The products were separated by radial chromatography on silica gel using 1/3 EtOAc/petroleum ether as eluent.

2-Azido-4-(benzo[*d*]thiazol-2-yl)aniline (20): major product; mp 134−136 °C with decomposition; IR 3384, 2115, 1618, 1476, 1435, 1315, 1276 cm^{-1}; ^1H NMR (500 MHz, CD_2Cl_2) δ 4.24 (2H, s), 6.76 (1H, d, J = 8.3 Hz), 7.35 (1H, t, J = 7.7 Hz), 7.46 (1H, t, J = 7.5 Hz), 7.63 (1H, dd, J = 8.2, 1.7 Hz), 7.85 (1H, d, J = 1.7 Hz), 7.89 (1H, d, J = 8.0 Hz), 7.97 (1H, d, J = 8.1 Hz); ^{13}C NMR (125.8 MHz, CD_2Cl_2) δ 115.0 (6.76), 117.1 (7.85), 121.5 (7.89), 122.5 (7.97), 124.3, 124.7 (7.35), 125.5, 125.6 (7.63), 126.2 (7.46), 134.7, 141.2, 154.2, 167.3; HRMS (ES, positive) $C_{13}H_{10}N_5S$ (M + H) calcd 268.0657, found 268.0645. **2-Phenylbenzo[*d*]thiazole (21):** minor product; characterized by comparison to an authentic sample.[49]

Reaction with d-G. A 500 mL volume of the pH 7.1 phosphate buffer containing 10 mM d-G was incubated at 30 °C, while 20 mL of a 25 mM solution of **8** in CH_3CN was added in 1 mL portions every 6 min. After the last addition, the reaction was incubated for 30 min. The reaction mixture was extracted with CH_2Cl_2 (2 × 100 mL). After extraction, an insoluble brown precipitate formed in the buffer. After cooling in an ice−water bath, this material was removed from the buffer by vacuum filtration. The precipitate was washed several times with CH_2Cl_2 and with small amounts of cold water to yield 35 mg (28% yield) of product that was pure by HPLC analysis (C-8 reverse phase column, 70/30 MeOH/H_2O eluent, 1 mL/min, UV absorbance at 212 and 340 nm).

***N*-(2′-Deoxyguanosin-8-yl)-4-(benzo[*d*]thiazol-2-yl)aniline (28):** mp 236−240 °C with decomposition; IR 3183, 1679, 1640, 1592, 1559, 1539, 1180, 1075, cm^{-1}; ^1H NMR (500 MHz, DMSO-d_6) δ 2.04 (2H, dd, J = 12.8, 5.4 Hz), 3.78 (2H, s), 3.94 (1H, s), 4.44 (1H, d, J = 5.2 Hz), 5.36 (1H, br s), 6.03 (1H, br s), 6.35 (1H, dd, J = 9.4, 5.8 Hz), 6.42 (2H, s), 7.40 (1H, t, J = 7.4 Hz), 7.50 (1H, t, J = 7.3 Hz), 7.90 (2H, d, J = 8.7 Hz), 8.01 (3H, m), 8.09 (1H, d, J = 7.9 Hz), 9.07 (1H, s), 10.62 (1H, br s); ^{13}C NMR (125.8 MHz, DMSO-d_6) δ 38.4 (2.04), 61.2 (3.78), 71.1 (4.44), 82.7 (6.35), 87.0 (3.94), 112.1, 117.1 (7.90), 121.9 (8.09), 122.1 (8.01), 124.8 (7.40), 126.2 (7.50), 127.7 (8.01), 133.9, 142.1, 143.5, 149.4, 152.8, 153.5, 155.5, 167.1; HRMS (ES, positive) $C_{23}H_{21}N_7O_4SNa$ (M + Na) calcd 514.1273, found 514.1276.

4-(Benzo[*d*]thiazol-2-yl)benzenediazonium tetrafluoroborate (26): A 1.0 mmol (0.226 g) sample of **1** was dissolved in 3 mL of absolute EtOH. After stirring for 10 min, dropwise addition of 0.5 mL of 48% HBF_4 yielded a clear dark yellow solution. The reaction mixture was immersed in an ice−salt water bath at −10 °C. After 15 min, 0.25 mL of isoamyl nitrite was added to the stirred reaction mixture in a dropwise fashion. The reaction mixture was stirred for 45 min at −10 °C. Addition of 20 mL of Et_2O generated a yellow precipitate. Vacuum filtration yielded 312 mg (96%) of crude product. Recrystallization of a 100 mg sample from DMF/CCl_4 yielded 60 mg of product: mp 128−130 °C with decomposition; IR 3099, 3057, 2289, 1579, 1468, 1317, 1025, 828, 765 cm^{-1}; ^1H NMR (500 MHz, DMSO-d_6) δ 7.59 (1H, t, J = 7.6 Hz), 7.65 (1H, t, J = 7.4 Hz), 8.2 (1H, d, J = 8.0 Hz), 8.29 (1H, d, J = 7.9 Hz), 8.65 (2H, d, J = 8.8 Hz), 8.81 (2H, d, J = 8.8 Hz); ^{13}C NMR (125.8 MHz, DMSO-d_6) δ 117.0, 123.0, 124.0, 127.3, 127.6, 129.2, 134.0, 135.8, 142.5, 153.5, 163.6.

Reduction of 26 by $NaBH_4$ in Phosphate Buffer. The diazonium salt (20 mg, 0.06 mmol) was dissolved in 15 mL of the pH 7.1 phosphate buffer. $NaBH_4$ (0.15 g, 4 mmol) was added to the reaction mixture. The mixture was incubated for 4 h at 30 °C with occasional stirring. The reaction medium was extracted with CH_2Cl_2 (3 × 10 mL). The combined extracts were dried (Na_2SO_4), filtered, and rotary evaporated to obtain a yellowish brown solid. The product mixture was characterized by HPLC coinjection (conditions same as above) with standard samples of **1** and **21** and by comparing the ^1H NMR spectrum of the mixture with those of the standards. Yields of the products were determined by HPLC and ^1H NMR.

Kinetics and Trapping Experiments with d-G. Kinetics experiments were carried out at 30 °C in the pH 7.1 0.02 M phosphate buffer containing 2.5, 5.0, and 10.0 mM d-G. Solutions were incubated in cuvettes in the thermostatted cell holder of a UV−vis spectrophotometer for ca. 20 min before kinetic runs were initiated by injecting 15 μL of a 5.0 mM solution of **8** in CH_3CN into 3 mL of the buffer to obtain an initial concentration of **8** of 2.5×10^{-5} M. Data were collected at 314 and 344 nm. Absorbance versus time data were fit to a first-order rate equation at all wavelengths.

A series of d-G solutions in the concentration range of 0.25 to 5.0 mM were prepared in the pH 7.1 0.02 M phosphate buffer. Solutions were incubated at 30 °C in Teflon-capped round-bottom glass vials for ca. 20 min before 15 μL of a 5.0 mM solution of **3** in CH_3CN was added to 3 mL of the buffer. A control experiment in phosphate buffer in the absence of d-G

(49) Pal, S.; Patra, G.; Bhunia, S. *Synth. Commun.* **2009**, *39*, 1196–1203.

was also included. Reaction mixtures were analyzed in duplicate after 3 h by 20 μL injections of each reaction mixture onto an HPLC (conditions the same as above). Product peak areas were plotted against [d-G].

Calculations. Density functional calculations were carried out using the Gaussian 03[50] and SPARTAN 08[51] suites of programs. Geometry optimization of the ground state nitrenium ions **11** and **12** and the quinolimines **16** and **19a** was executed at the B3LYP/6-31G(d) level, and their verification as minima employed harmonic frequency analyses, which afforded all real frequencies. Calculations at the same level for **13**, **14**, **15**, and **18** were previously reported.[37] For visual comparisons, EDEP surfaces of **11** and **13** were calculated at 0.002 electrons/au^3, and LUMO properties of both ions were computed at a static isovalue of 0.032. Isodesmic reaction energies were computed using electronic energies without inclusion of zero point corrections.

(50) Frisch, M. J. et al. *Gaussian 03*, revision E.01; Gaussian, Inc.: Wallingford, CT, 2005.

(51) *Spartan '08 for Macintosh*, version 1.2.1; Wavefunction Inc.: Irvine, CA, 2008.

Acknowledgment. We thank the NIH/NIGMS (Grant No. R15 GM088751-01) for support of this work. K.J.J. thanks the College of Arts and Science of Miami University for a Dean's Scholar award.

Supporting Information Available: Table S1, containing all individual rate constants measured by uv methods; Figure S1, containing all rate constants measured by HPLC; Figure S2, containing the absorbance vs pH titration curve for **8**; Figure S3, containing the LUMOs of **11** and **13**; Quick Time movies of the LUMOs and EDEP surfaces of **11** and **13**; Tables S2−S5, containing the *Z*-matrices for the optimized structures of **11**, **12**, **16**, and **19a** at the B3LYP/6-31G(d) level of theory; ^{1}H and ^{13}C NMR spectra for **20**, **26**, and **28**; HMQC spectra for **20** and **28**; and complete ref 50. This material is available free of charge via the Internet at http://pubs.acs.org.